29th EPS Conference on Plasma Phys. and Contr. Fusion Montreux, 17-21 June 2002 ECA Vol. **26B**, P-5.083 (2002)

Analysis of Pellet Toroidal Deflection in Sawtoothing Discharges

V Waller†, B Pégourié†, G Giruzzi†, G T A Huysmans†, L Garzotti‡ and A Géraud†

† *Association Euratom-CEA, C. E. Cadarache F-13108 Saint-Paul-Lèz-Durance*
‡ *Consorzio RFX, Corso Stati Uniti 4, I-35127 Padova*

Introduction

The injection of cryogenic hydrogen isotope pellets is in many ways the best candidate for particle-refueling of high-performance discharges. It also proved to provide a powerful diagnosis of the hot plasma. In particular, information on the current distribution (or q profile) have been obtained from the analysis of the structure of the ablation pattern [1] and of the pellet trajectory [2]. Indeed, pellets are deflected in the counter-current direction when injected in tokamak discharges. This deflection is due to a rocket effect associated with the Spitzer-Härm distortion of the electron distribution. The weak asymmetry in the energetic part of the electron distribution leads to an imbalance of ablation between the counter-current and co-current sides, resulting in a net toroidal force that is the cause of the pellet acceleration. The trajectory reflects therefore the current density distribution (more precisely, the asymmetry of the distribution function) across the discharge during the pellet lifetime (few hundreds of μs).

From an experimental point of view, sawtooth activity is not affected by the injection of a pellet if it remains outside the $q = 1$ magnetic surface. In this case, the induced cooling is quasi-adiabatic. Conversely, pellets penetrating $q = 1$ trigger systematically a non-adiabatic drop of the central electron temperature, identical to that observed during a sawtooth crash [3].

Experimental results

The experiments have been performed in Tore Supra (major radius $R_0 = 2.4$ m, minor radius $a = 0.8$ m, circular cross-section), which is equipped with a single-shot, high-speed, pneumatic injector launching hydrogen or deuterium pellets at velocities up to 3500 m.s^{-1}, high enough to allow central penetration. For macroscopically similar experimental conditions, pellet trajectories display significant differences when crossing $q = 1$, see Figs. 1a and 1c. Pellets are injected from the right (midplane, low field side), $D\Phi$ is the toroidal direction and R the major radius. The path of the pellet and its surrounding neutral cloud corresponds to the central dark zone whose width is few millimeters. In Fig. 1a, the curvature of the pellet trajectory is always of the same sign whereas in Fig. 1c, the curvature is inverted at $R = 2.61$ m (location of $q = 1$) and almost straight afterwards.

The toroidal acceleration is given by the momentum conservation of the pellet-cloud system:

$$N_p \frac{dV_p}{dt} = \left(\frac{dN_p^{counter}}{dt} - \frac{dN_p^{co}}{dt} \right) U \left\langle \cos\left(\theta\right) \right\rangle$$

where N_p is the particle content of the pellet, $dN_p^{counter} / dt$ and dN_p^{co} / dt are the ablation rates on the counter and co-current sides, respectively, U is the expansion velocity of the ablatant [4] and $\left\langle \cos\left(\theta\right) \right\rangle = 1/2$ accounts for the projection of U on the field lines. The Neutral Gas and Plasma Shielding (NGPS) model [5] used for the calculation of the ablation rates takes explicitly into account the shape of the electron and ion distribution functions. Here, the Braginskii approximation of the electron distribution function with current is used [6].

Main characteristics of discharges TS12635 and TS12637 (Fig. 1) are: central temperature $T_e(0) = 2$ keV, density $n_e(0) = 4 \times 10^{19}$ m^{-3}, ohmic current $I_P = 1.4$ MA and loop voltage

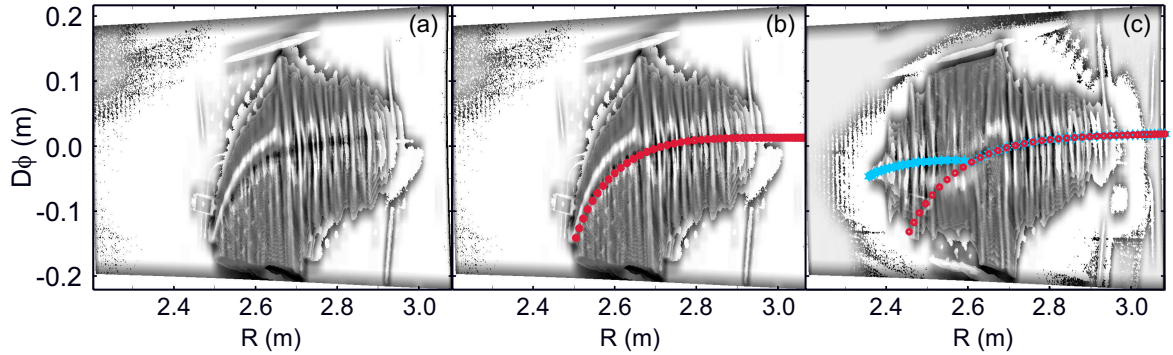

Figure 1: [Pellet TS12635] (a) Reprocessed time-integrated CCD image of the ablation pattern . The pellet is injected from right to left in the tokamak midplane. $D\phi$ is the toroidal direction and R the major radius. (b) Same picture with the calculated trajectory superimposed (red markers). [Pellet TS12637] (c) The trajectories are calculated with the current densities displayed in Fig. 3b: unperturbed trajectory (red markers), perturbed trajectory (blue markers).

$V_{loop} = 1$ V. The values of the safety factor are: $q(a) = 3.1$ and $q(0) = 0.9$ ($q = 1$ at $R = 2.61$ m in the midplane, low field side). The effective charge $Z_{eff} \approx 1.2$ is assumed to be constant. The hydrogen pellets are injected at a velocity $V_p = 1500$ m.s^{-1} and contain 9.5×10^{20} atoms. The reconstructed trajectories are superimposed on the images in Figs. 1b and 1c (red markers). If the agreement is satisfactory in the former case, the discrepancy is obvious in the latter.

Twenty-five well-documented discharges with explicit sawtooth activity have been selected in the Tore Supra database. The range of pellet (both hydrogen and deuterium) parameters are: particle content $4 \times 10^{20} < N_p < 11 \times 10^{20}$ atoms, velocity $1300 < V_p < 3100$ m.s^{-1}. The corresponding plasma parameters at the end of the pellet path are: $3 \times 10^{19} < n_e\,(\lambda_p) < 7.5 \times 10^{19}$ m^{-3} for the density and $1.7 < T_e\,(\lambda_p) < 3.0$ keV for the temperature, with various locations of the $q = 1$ surface ($2.47 < R_{q=1} < 2.69$ m) and values of the plasma current ($1.0 < I_p < 1.7$ MA).

A suitable parameter for characterizing the perturbation is the angle between the perturbed and unperturbed trajectories (i.e. the experimental trajectory and that calculated with the equilibrium current profile). Its tangent is equal to Δ/Λ where Δ and Λ are described in the insets of Fig. 2b. The result is plotted as a function of $\delta t = t_{lc} + \pi_{st} - t_p$ (see Fig. 2a). Two groups

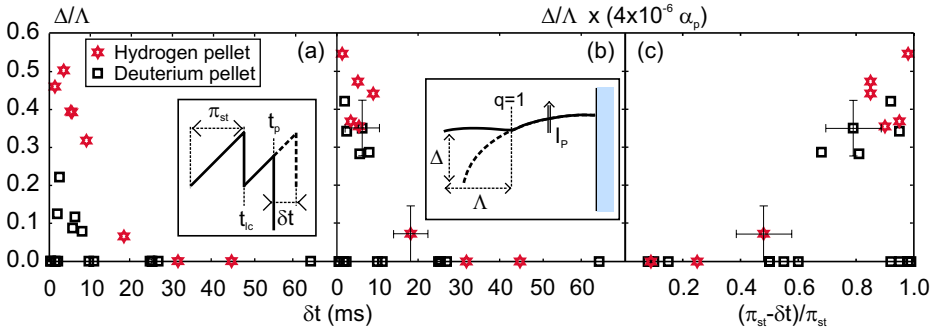

Figure 2: (a) Δ/Λ vs. $\delta t = t_{lc} + \pi_{st} - t_p$. (b) $\alpha_p \Delta/\Lambda$ vs. δt. The factor α_p takes into account the differences between the initial pellet parameters. Δ, Λ and δt are described in the two insets. (The factor 4×10^{-6} is for the convenience of the display.) (c) $\alpha_p \Delta/\Lambda$ vs. $(\pi_{st} - \delta t)/\pi_{st}$.

of points can be distinguished depending on the pellet material and injection parameters. One can correct their effect using the ablation scaling and assuming a constant acceleration inside $q = 1$. This yields a correction factor equal to $\alpha_p = r_p^{5/3} M_0^{5/6} V_p^2/\Lambda$ where r_p is the pellet initial radius and M_0 the mass number of the pellet material. In Fig. 2b, $\alpha_p \Delta/\Lambda$ is displayed versus δt showing a unique trend in the cloud of points. The main results are: (i) that the occurrence of the perturbation is limited to a short time interval close to the expected crash ($\delta t \lesssim 10$ ms) and (ii) that, in this area, the major part of trajectories (65%) is significantly perturbed. The magnitude of the perturbation and the evidence of a reversal of the ablation asymmetry on $q = 1$ (i.e. a negative perturbation of the current distribution) is reminiscent of a magnetic reconnection phenomenon. The simultaneity with the pellet crossing suggests that the pellet is the cause of this so-called sawtooth crash. Also, $\alpha_p \Delta/\Lambda$ is displayed in Fig 2c versus the phase of the pellet injection with respect to the sawtooth, $(\pi_{st} - \delta t)/\pi_{st}$, showing a possible correlation between the importance of the perturbation and the development of a precursor.

Candidate explanation

Along the pellet path the pressure profile is transiently perturbed because, during homogenization, part of the energy is stored as kinetic energy in the expanding cold blob. The pressure profile is thus transiently pinched just in front of the ablation cloud and flattened at the cloud location. This phenomenon is amplified close to rational surfaces due to the poloidal localization of the perturbation.

On Tore Supra, the sawtooth crash is triggered by the onset of the resistive internal kink mode. It is destabilized by the gradient of the current density and stabilized by the diamagnetic drift (i.e. by the pressure gradient). When the ablation cloud reaches $q = 1$, the associated local flattening of the pressure lowers the instability threshold what triggers the onset of the internal kink (it can be shown that the transient peaking of the pressure is insufficient to destabilize the ideal kink). With unperturbed plasma parameters, the inverse of the growth rate λ of the resistive kink is ≈ 100 μs. Taking into account the increase of the resistivity η due to the cooling of the plasma by the pellet (typically $\times 30$ in our case), one finds $\lambda^{-1} \approx 30$ μs (since $\lambda \propto \eta^{1/3}$). This value is close to the time required for the pellet to reach $q = 1$: a few R_p/V_p, i.e. $= 15 - 30$ μs, where R_p is the radius of the ablation cloud (typically 10^{-2} m). It follows that the pellet itself crosses the $q = 1$ surface and penetrates the plasma core at the end of the reconnection process.

Comparison with experiments

This scenario has been tested on pellet TS12637, which presents the most significant perturbation. On $q = 1$, the perturbation of the trajectory is characterized by a reversal of the curvature associated with a negative current layer. A Fokker-Planck calculation [7] has been performed to compute the electron distribution that corresponds, starting from the equilibrium Spitzer-Härm function (equilibrium current density $J = 1.8$ MA.m^{-2}) and applying a dc electric field E during a time τ. A value $E = 2.6$ V.m^{-1} is necessary for fitting the experimental inflection of the trajectory (as long as τ is shorter than the collision time, only the product $E\tau \approx 8 \times 10^{-5}$ V.s.m^{-1} is constrained). The resulting distribution function, carrying a current density equal to -23 MA.m^{-2}, is displayed in Fig. 3a. For comparison, the Maxwellian and equilibrium Spitzer-Härm distributions are also plotted. This calculation has been done for a current layer of infinitesimal thickness. As soon as a finite radial extent δ_r of the current

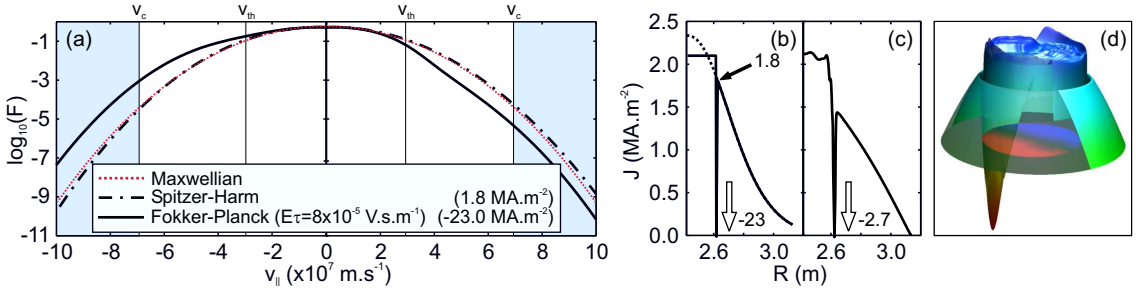

Figure 3: (a) Electron distribution functions vs. parallel velocity. Maxwellian (dotted line), Spitzer-Härm (dashed-dotted line), Fokker-Planck ($E\tau \approx 8 \times 10^{-5}$ V.s.m^{-1}). The thermal and critical velocities, v_{th} and v_c, are specified. (b) Current densities used in trajectory simulations (dotted line: unperturbed distribution; solid line: perturbed distribution) vs. major radius R. (c) Current density at the location of the negative peak in Fig. 3d. (d) Current density distribution in a poloidal cross-section at the maximum of the perturbation.

perturbation is considered, the electric field must be decreased by a factor $(1 + \delta_r/R_p)^{-1}$. In the inner of $q = 1$, the consequence of the magnetic reconnection is to deplete the energetic electrons [8]. A convenient way to describe the associated distribution function is to truncate the equilibrium Spitzer-Härm distribution at some critical velocity v_c. To reproduce the experimental curvature of the trajectory (Fig. 1c, red markers), a value $v_c \approx 5.5 \times 10^7$ m.s^{-1} must be taken ($v_c/v_{th} \approx 2.3$). The current density carried by this distribution is 2.1 MA.m^{-2}. This corresponds to a constant safety factor $q = 1$ in the whole plasma core, i.e. to a full reconnection. The current density that follows is shown in Fig. 3b. The uniqueness of this solution is not assessed because experiments constrain only a momentum of the electron distribution function through ablation asymmetry. The robustness of our results have been thus tested, showing that the distribution function presented in Fig 3a corresponds to the minimum perturbation of the equilibrium current density.

For comparison, 3D MHD calculations have been performed with the code described in [9]. The time evolution of the resistive internal kink mode has been calculated using the characteristics of discharge TS12637, the resistivity being increased to take into account the cooling of the plasma by the pellet. The current distribution at the maximum of the mode evolution is shown in Fig. 3d and a radial profile at the location of the negative peak in Fig. 3c. A good qualitative agreement is observed between the two calculated J profiles of Figs. 3b and 3c. It must be noticed that the poloidal extension of the negative current layer $\delta_\theta/(2\pi) \approx 10^{-1}$ is significantly smaller than the proportion of abnormally deflected pellets (65% in the time interval of interest). This is a further confirmation that the pellet triggers the crash.

References

[1] TFR group, Europhys. Lett. **2**, 267 (1986).
[2] L. Garzotti *et al.*, Phys. Rev. Lett. **84**, 5532 (2000).
[3] D. F. da Cruz *et al.*, Phys. Rev. Lett. **75**, 3685 (1995).
[4] P. B. Parks and R. J. Turnbull, Phys. Fluids **21**, 1735 (1978).
[5] V. Waller *et al.*, in *Controlled Fusion and Plasma Physics: Proceedings of the 28th European Conference, Madeira, Portugal, 2001* (European Physical Society, Funchal, 2001).
[6] B. V. Kuteev, Nucl. Fusion **35**, 431 (1995).
[7] R. Dumont, G. Giruzzi and E. Barbato, Phys. Plasmas **7**, 4972 (2000).
[8] R. Jasper *et al.*, Phys. Rev. Lett. **72**, 4093 (1994).
[9] G. T. A. Huysmans *et al.*, Phys. Rev. Lett. **87**, 245002-2 (2001).